*33rd EPS Conference on Plasma Phys. Rome, 19 - 23 June 2006 ECA Vol.**30I**, P-1.153 (2006)*

Electron Bernstein Wave Heating and Emission in the TCV Tokamak

A. Mueck[1], Y. Camenen[1], S. Coda[1], L. Curchod[1], T.P. Goodman[1], H.P. Laqua[2],
K. Mason[1], R. Patterson[1], A. Pochelon[1], L. Porte[1], V.S. Udintsev[1]

[1] *Ecole Polytechnique Fédérale de Lausanne (EPFL),*
Centre de Recherches en Physique des Plasmas, Association EURATOM, CH-1015 Lausanne
[2] *Max-Planck-Institut für Plasmaphysik, Assoziation EURATOM, D-17491 Greifswald*

Electron cyclotron heating of high density plasmas is limited due to so-called wave cut-offs. The double mode conversion scheme from O-mode to X-mode and finally to Bernstein mode O-X-B offers the possibility to overcome this limit [1]-[4]. At a particular launching angle, an O-mode wave converts to X-mode at the plasma cut-off. The power transmission function T from O- to X-mode was derived in [5] and defines the angular window for the O-X conversion

$$T(N_\perp, N_\parallel) = exp\left(-\pi k_0 L_n (Y/2)^{1/2}\left[2(1+Y)(N_{\parallel,opt}-N_\parallel)^2 + N_\perp^2\right]\right) \quad (1)$$

with the density scale length L_n, the refraction indices $N_\perp$, $N_\parallel$ and $Y = \omega_{ce}/\omega$ with the electron cyclotron frequency ω_{ce}. Only for the optimum $N^2_{\parallel,opt} = Y/(Y+1)$, equivalent to an optimum injection angle, the O-mode wave can be completely converted to X-mode. In the Tokamak à Configuration Variable (TCV), second harmonic Electron Cyclotron Resonance Heating (ECRH) at 82.7 GHz is the main heating source. The power of six gyrotrons with 500 kW each can be injected at chosen angles from four upper lateral and two equatorial ports. Reflected EC power, the EC stray radiation, is measured via semiconductor diodes, installed in several sectors of TCV.

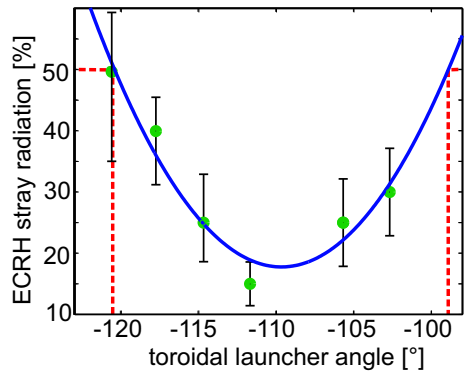

Figure 1: *EC stray radiation level for a toroidal launcher angle scan. A clear minimum in the stray radiation is visible, equivalent with a maximum in EC power absorption.*

At a standard TCV magnetic field of B=1.5 T, the plasma becomes overdense to second harmonic X-mode for electron densities of $n_e \approx 4.2 \cdot 10^{19}$ m^{-3} and to O-mode injection at $n_e \approx 8.7 \cdot 10^{19}$ m^{-3}. To achieve a large angular window, the density scale length at the plasma cut-off has to be short. Steep density gradients were realized in TCV H-modes with central electron densities of $n_e \approx 1.5 \cdot 10^{20}$ m^{-3}, low q, high triangularity and magnetohydrodynamic activity like Edge Localized Modes (ELMs) and sawteeth. At these densities, the plasma cut-off is placed at $\rho_\psi \approx 0.9$, at the steep edge density gradient region of the H-mode.

To show experimentally the angle dependence of the power transmission from O- to X-mode, an angle scan was performed, injecting modulated ECRH with a low duty cycle of 6%, to avoid the triggering of ELMs. In figure 1, the EC stray radiation level for a toroidal launcher angle scan is shown. A clear minimum in the stray radiation is visible, equivalent to a maximum in EC power

absorption, as expected. The same angle dependence of the stray radiation level is observed for the poloidal angle and, as well, for launching from an equatorial or from an upper lateral port. To compare the experimental results with simulations, the optimum angle was calculated with the ray tracing code ART [6] for ray propagation and absorption, including O-X-B mode conversion. The calculated optimum angle is within only 2^o from the experimentally determined angle, showing good agreement [7]-[9].

The duty cycle of the injected ECRH was increased to 46% to show EBWH at the optimum angle. For nearly equatorial launch, the simulated deposition location is with $\rho_\psi \approx 0.3$ close to the plasma center. The global absorption can be determined to 60% via the diamagnetic loop (DML) [10]. Switching from O- to X-mode injection, the power absorption reduces to less than

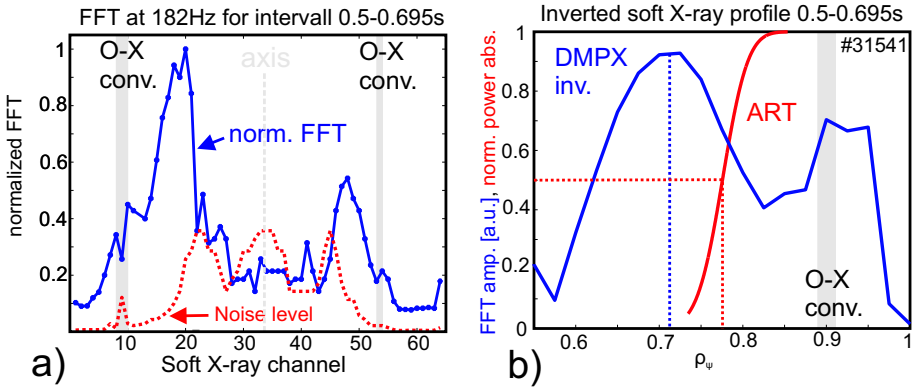

Figure 2: *a) FFT amplitude at ECRH modulation frequency for all 64 soft X-ray channels. Two clear maxima are visible, marking the EBW deposition location. b) FFT amplitude of inverted soft X-ray (DMPX) time traces over* ρ_ψ. *The experimental deposition is found at* $\rho_\psi \approx 0.72$, *the calculated location, where half of the beam power is absorbed, is at* $\rho_\psi \approx 0.78$.

10%. Since the absorption of the X-mode is very low, a large fraction of multipass absorption in O-mode outside the cut-off layer can be excluded. However, due to strong interference of the sawtooth instability, the location of the power deposition is difficult to resolve. By injecting the EC waves via an upper lateral launcher, the simulated deposition location was positioned at $\rho_\psi \approx 0.78$, well inside the plasma cut-off at $\rho_\psi \approx 0.9$ and outside the area, strongly influenced by the sawteeth. In the soft X-ray time traces, measured via a high spatial resolution wire chamber (DMPX), a clear response to the modulated ECRH is visible already by the nacked eye. To determine the deposition location, an FFT is made of each of the 64 radial DMPX channels. In figure 2a) the FFT amplitude at the ECRH modulation frequency is drawn over the DMPX channels. Two clear maxima are visible, indicating the EBW deposition. Since the soft X-ray signals are line-integrated, the DMPX time traces have to be inverted to find the actual deposition location. In figure 2b) the FFT amplitude of the tomographically inverted DMPX signals is drawn over the normalized flux coordinate ρ_ψ. A clear maximum is seen at $\rho_\psi \approx 0.72$, marking the

deposition location. The calculated location, where half of the injected beam power is absorbed, is found at $\rho_\psi \approx 0.78$, within only 10% of the experimentally determined deposition location.

To be able to show an increase in the electron temperature due to EBWH, long pulses of 100 ms

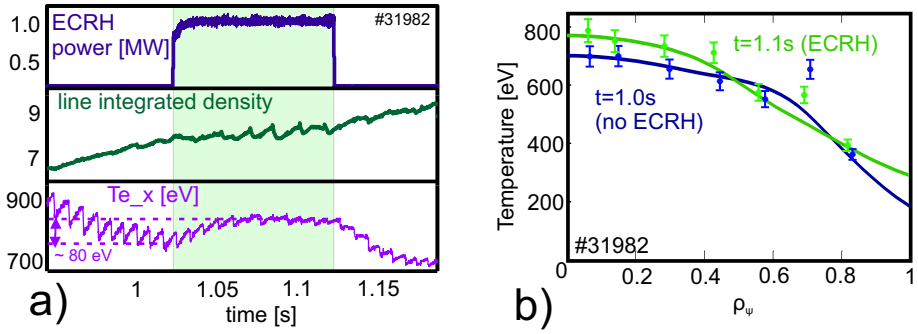

Figure 3: *a) ECRH pulses of 100 ms were injected. The temperature, measured via the soft X-ray absorber method, shows an increase of $\Delta T_e \approx 80$ eV. The quasi-constant density emphasizes the relevance of the temperature measurement. b) The central development of the Thomson temperature profiles before ($t = 1.0$ s) and during ECRH pulse ($t = 1.1$ s) supports the result of the soft X-ray measurement.*

were injected, as shown in figure 3a). The temperature measurement via the soft X-ray absorber method evaluates an increase of $\Delta T_e \approx 80$ eV, seen in all channels. The quasi-constant density emphasizes the validity of the temperature measurement. In figure 3b), the Thomson temperature profiles before ($t = 1.0$ s) and during ECRH pulse ($t = 1.1$ s) are seen. The temperature increase during the EC pulse supports the results of the soft X-ray temperature measurement.

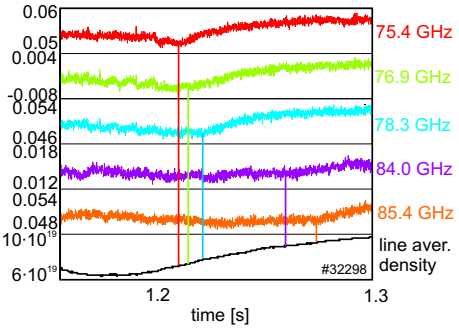

Figure 4: *First EBE measurements for several frequencies. As expected, the EBE onset density increases with the frequency.*

f [GHz]	cut-off, calc. $[10^{19}\mathrm{m}^{-3}]$	FIR $[10^{19}\mathrm{m}^{-3}]$	n_e, on axis $[10^{19}\mathrm{m}^{-3}]$
75.4	7.0	6.7	6.8
76.9	7.4	7.1	7.3
78.3	7.6	7.5	7.7
84.0	8.8	9.1	9.7
85.4	9.1	9.5	10

Table: *Comparison between calculated O-mode cut-off densities for different frequencies and line-integrated and Thomson measurements of the EBE onset densities.*

First Electron Bernstein Emission measurements were performed with a newly installed equatorial launcher with steerable mirrors for reception measurements. The launcher is connected to the ECE system via an open 1 inch waveguide line. In figure 4, first EBE measurements are presented for several frequencies. A clear emission signal is observed on all channels for an overdense plasma, observed at an optimum angle. As expected, the EBE onset density, com-

parable with the cut-off density, increases with frequency. In the table, the calculated onset for various frequencies is compared with a high resolution line-integrated density measurement (FIR) and the Thomson density on axis. The measured EBE onset densities are in good agreement with the calculated cut-off densities, the error is very low, only $\sim$ 5-10%.

Conclusions

The optimum injection angle for O-X-B conversion was determined experimentally. A clear angle dependence in the EC stray level was found. Simulations with the ART code were performed and the simulated optimum angle is within 2^o in good agreement with the measurements. Global absorption of the order of 60% was observed with the diamagnetic loop for modulated ECRH power injection. The local deposition, determined by FFT analysis of inverted soft X-ray data, was well inside the plasma cut-off layer at $\rho_\psi \approx 0.72$, and lies within only 10% of the simulated beam absorption at $\rho_\psi \approx 0.78$. For long ECRH pulses, a temperature increase of $\Delta T_e \approx 80$ eV was measured consistently by Thomson scattering and the soft X-ray absorber method. First Electron Bernstein wave emission measurements were presented, reproducing the cut-off density at the EBE onset for several frequencies within 10%. In summary, localized heating experiments were presented, demonstrating EBWH for the first time via the O-X-B mode conversion process in a standard aspect ratio tokamak.

References

[1] T.H. Stix, Waves in Plasmas, Springer-Verlag New York, Inc., 1992

[2] J. Preinhaelter, V. Kopecký, J. Plasma Physics **10**, part 1 (1973), pp 1-12

[3] I. Bernstein, Phys. Rev. Lett. **109**, 10 (1958)

[4] H.P. Laqua et al., Phys. Rev. Lett. **78**, 3467 (1997)

[5] E. Mjølhus et al., Plasma Phys. **31**, 7 (1984)

[6] F. Volpe, Electron Bernstein emission diagnostic of electron temperature profile at W7-AS Stellarator, PhD thesis, IPP Garching and Greifswald, IPP Report 13/1, March 2003

[7] A.Mueck et al., O-X-B Mode Conversion in the TCV Tokamak, Proc. 32nd Eur. Conf. on Plasma Phys. and Contr. Fusion (Tarragona, 2005), P4.110

[8] A.Mueck et al., Electron Bernstein Wave Heating in the TCV Tokamak, 47th Annual Meeting of the Division of Plasma Physics (Denver 2005), FP1.00062

[9] A.Mueck et al., Electron Bernstein Wave Heating in the TCV Tokamak, Fourteenth Joint Workshop on Electron Cyclotron Emission and Electron Cyclotron Heating, Greece, 2006

[10] A. Manini, J.-M. Moret et al., Plasma Phys. Control. Fusion **44** (2002) 139-157

The ART software has been acquired and used with kind permission of F. Volpe and IPP-Garching. This work is partly funded by the 'Fonds National Suisse pour la recherche scientifique'. A. Mück is supported by an EURATOM fellowship.